

Perturbativity Limits for Scalar Minimal Dark Matter with Yukawa Interactions: Septuplet

Chengfeng Cai^a, Ze-Min Huang^a, Zhaofeng Kang^b, Zhao-Huan Yu^{a,c,d},
and Hong-Hao Zhang^{a,1}

^a*School of Physics and Engineering, Sun Yat-Sen University, Guangzhou 510275, China*

^b*School of Physics, Korea Institute for Advanced Study, Seoul 130-722, Korea*

^c*Key Laboratory of Particle Astrophysics, Institute of High Energy Physics, Chinese Academy of Sciences, Beijing 100049, China*

^d*ARC Centre of Excellence for Particle Physics at the Terascale, School of Physics, The University of Melbourne, Victoria 3010, Australia*

Abstract

The candidate of minimal dark matter (MDM) is limited if one demands perturbativity up to a very high scale, and it was believed that the MDM model with a real scalar septuplet could keep perturbative up to the Planck or GUT scale. In this work we point out that it is not true after taking into account the running of the quartic self-couplings of the scalar septuplet. For the septuplet mass around 10 TeV, which is suggested by the observed dark matter relic abundance, these couplings would hit the Landau pole at a scale $\sim 10^8 - 10^9$ GeV, much lower than the Planck scale. We attempt to push up the Landau pole scale as high as possible by proposing an extension with extra Yukawa interactions of the septuplet. We find that in principle the Landau pole could be deferred to a scale of $\sim 10^{14}$ GeV if one could tolerate a serious fine-tuning of the initial condition of the Yukawa coupling. Moreover, if the MDM particle mass could be relaxed to $\sim 10^8$ GeV, which would need some nonthermal production mechanisms to give a correct relic abundance, the Landau pole scale could be pushed up above the Planck scale.

¹Email: zhh98@mail.sysu.edu.cn

Contents

1	Introduction	2
2	The Real Scalar Septuplet MDM Model	4
2.1	Details of the septuplet model	4
2.2	Several relevant phenomenologies	7
2.2.1	DM phenomenologies	7
2.2.2	Vacuum stability	9
3	Confronting perturbativity	10
3.1	Perturbativity bound on the septuplet model	11
3.2	Push up the Landau pole scale in the 7-3-5 model	13
3.2.1	The 7-3-5 model	13
3.2.2	How high can the Landau pole scale be?	15
3.2.3	Constraints from perturbativity and VS in the $F_0 = 0$ case . .	18
3.2.4	Towards the Planck scale: relaxing the septuplet mass	20
3.3	Analytical treatments	21
3.3.1	$F_0 = 0$	21
3.3.2	$F_0 > 0$	23
4	Conclusions and discussions	25

1 Introduction

Among a large pool of dark matter (DM) models, the minimal dark matter (MDM) model [1] is of special interest. There are extensive studies on its implication for DM relic abundance [1–4] and its predictions for direct detection [1–6], indirect detection [1–5, 7–10], and collider [1, 3, 6, 11–15] experiments. A MDM particle is the electrically neutral component of a $SU(2)_L \times U(1)_Y$ multiplet in a high dimensional representation, which is denoted as $(2j + 1, Q_Y)$ with j the half integer and Q_Y the hyper charge. Minimally, MDM annihilations only involve gauge interactions. As a consequence, the MDM particle mass can be predicted from the observed DM abundance. Moreover, it may shed light on the mechanism of DM stability by virtue of an accidental symmetry rather than an artificial protecting symmetry. As long as the dimension of the representation is sufficiently high, the electroweak gauge symmetries could forbid any coupling between the MDM and the standard model (SM) particles which can lead to the MDM decay, at tree or even at nonrenormalizable level. For instance, a fermionic MDM particle in $(5, 0)$ can be

stable up to dimension-6 operators. The quintuplet MDM has been well studied in Refs. [1–3, 9, 10, 15].

Another option is a real scalar septuplet $(7, 0)$ ² which, to our knowledge, was less studied [4–6, 10, 12], in particular on its self-consistency in the framework of quantum field theory. The observed DM relic abundance suggests that this septuplet MDM particle has a threshold mass of ~ 8 TeV (or ~ 22 TeV) without (or with) including the Sommerfeld enhancement (SE) effect [4, 5]. In this paper we revisit this DM candidate in light of some recent progresses, in particular the work in Ref. [17], which for the first time systematically calculated the beta functions of quartic couplings of MDM and found out that they have deep implications to the perturbativity of the model. Previously, the perturbativity was only checked with respect to gauge couplings, concretely g_2 , and it was claimed the septuplet MDM model can keep perturbative up to the Planck scale [1] (but it was recently lowered down to the GUT scale after including two-loop contributions [16]). Nevertheless, a renormalization group equation (RGE) study on the MDM quartic self-interaction couplings shows that they will hit the Landau pole (LP) at a scale merely around 10^8 GeV [17], much faster than gauge couplings.

In this article we attempt to defer the appearance of the Landau pole by introducing sizable Yukawa interactions of the septuplet MDM. It is found that the most helpful case is the existence of a coupling of the scalar septuplet to a fermion triplet and a fermion quintuplet. If the two fermion multiplets are active around 100 TeV, the perturbativity can be kept up to around $\Lambda_{LP} \simeq 10^{14}$ GeV. As a bonus of our scheme, the fermion triplet can be used to explain neutrino mass origin via the type-III seesaw mechanism³ [18]. Careful studies, both numerical and analytical, show that it is at the price of serious fine-tuning on the initial conditions. Relaxing the MDM particle mass to 10^8 GeV, under the assumption that the observed relic density is obtained in other ways, the model can even be perturbative near the Planck scale.

Other aspects of the septuplet MDM model are also investigated, and some of them are new. Different to fermionic MDM, scalar MDM couplings to the Higgs field are always allowed. If these couplings are significant they may alter physics associating with the Higgs, e.g., electroweak vacuum stability. We have to guarantee that the electroweak vacuum is indeed the global minimum in the presence of a scalar septuplet. Thus we figure out the vacuum stability (VS) conditions of the whole scalar potential, which are non-trivial owing to the complicated quartic couplings of

²Recently, a dimension-5 operator $\sim \Phi^3 H^\dagger H$ that violates the accidental Z_2 symmetry was pointed out by Ref. [16]. But this operator only induces DM decay at loop level.

³Of course, the realistic neutrino mixings require at least two triplets, but the other one is assumed to be very heavy for the sake of a Landau pole of g_2 as high as possible.

the septuplet. It is found that the electroweak vacuum can be absolutely stable at any scale below Λ_{LP} .

We organize the paper as follows. In Sec. 2 we introduce the septuplet MDM model and study several relevant phenomenologies. In Sec. 3 we investigate the perturbativity bound on the septuplet model as well as its extension with Yukawa interaction. Sec. 4 gives our conclusions and discussions.

2 The Real Scalar Septuplet MDM Model

In this section we begin by describing the model. We pay special attention to the scalar potential which is overlooked before. Then we investigate the perturbativity bound on the model including the evolution of quartic couplings of MDM self-interactions.

2.1 Details of the septuplet model

The MDM model was firstly proposed in Ref. [1]. The idea is to extend the SM with a colorless $SU(2)_L$ multiplet, whose electrically neutral component plays the role of the DM candidate. If the multiplet belongs to a representation with sufficiently high dimension, it would be unable to construct any renormalizable decay operator for this multiplet. Consequently, its neutral component could be stable and weakly couple to other particles.

Taking into account the nonrenormalizable operators, the DM stability condition sets a lower bound on the dimension of the representation n . The bound is $n \geq 5$ for fermionic multiplets and $n \geq 7$ for scalar multiplets. On the other hand, an upper bound on n can be determined by the perturbativity of the $SU(2)_L$ gauge coupling g_2 . It requires $n \leq 5$ for Majorana fermionic multiplets and $n \leq 8$ for scalar multiplets. Therefore, the minimal choice is a Majorana fermionic quintuplet with a hypercharge $Y = 0$, and the next-to-minimal extension is a real scalar septuplet with $Y = 0$. Note that for Dirac fermionic and complex scalar multiplets, $Y \neq 0$ leads to the spin-independent DM-nuclei scattering through the Z boson exchange and can be easily excluded by current direct detection experiments.

General discussions for a model with an extra $SU(2)_L$ scalar multiplet whose neutral component is a DM candidate can be found in Ref. [4]. Here we briefly revisit the real scalar septuplet case. The scalar septuplet Φ can be expressed as

$$\Phi = \frac{1}{\sqrt{2}}(\Delta^{(3)}, \Delta^{(2)}, \Delta^{(1)}, \Delta^{(0)}, \Delta^{(-1)}, \Delta^{(-2)}, \Delta^{(-3)})^T, \quad (1)$$

where $(\Delta^{(Q)})^* = \Delta^{(-Q)}$. The gauge covariant derivative of the septuplet with $Y = 0$

is

$$D_\mu \Phi = \partial_\mu \Phi - ig_2 W_\mu^a \tau^a \Phi, \quad (2)$$

where τ^a is the $SU(2)$ generators in the 7-dimensional representation. They satisfy the $su(2)$ algebra, i.e., $[\tau^a, \tau^b] = i\epsilon^{abc}\tau^c$. As usual, we choose the spherical basis and $\tau^3 = \text{diag}\{3, 2, 1, 0, -1, -2, -3\}$. It is convenient to define the ladder operators $\tau^\pm = \tau^1 \pm i\tau^2$. Since $W_\mu^\pm \equiv (W_\mu^1 \mp iW_\mu^2)/\sqrt{2}$ and $W_\mu^3 = \sin\theta_W A_\mu + \cos\theta_W Z_\mu$ with θ_W denoting the Weinberg angle, we have

$$W_\mu^a \tau^a = (s_W A_\mu + c_W Z_\mu) \tau^3 + \frac{1}{\sqrt{2}} (W_\mu^+ \tau^+ + W_\mu^- \tau^-), \quad (3)$$

where $s_W \equiv \sin\theta_W$ and $c_W \equiv \cos\theta_W$. The commutators of these operators can be easily derived:

$$[\tau^+, \tau^-] = 2\tau^3, \quad [\tau^3, \tau^\pm] = \pm\tau^\pm. \quad (4)$$

Since all $SU(2)$ representations are pseudo-real, we can relate an n -dimensional representation to its complex conjugate by a transformation matrix $T_{(n)}$:

$$T_{(n)} \tau^a T_{(n)}^{-1} = -(\tau^a)^*. \quad (5)$$

For the spherical basis $|e_k^{(n)}\rangle$ (eigenstates of τ^3 in the n -dimensional representation), $T_{(n)}$ satisfies

$$T_{(n)} |e_k^{(n)}\rangle = \begin{cases} (-)^{n+1} |e_k^{(n)}\rangle, & k \geq 0; \\ |e_{-k}^{(n)}\rangle, & k < 0. \end{cases} \quad (6)$$

Thus $T_{(7)}$ is a 7×7 matrix whose minor diagonal elements are 1 and the rest elements are 0. The conjugate of Φ can be constructed as $\tilde{\Phi} = T_{(7)} \Phi^*$. Particularly, for a real scalar septuplet, $\tilde{\Phi} = \Phi$, which is consistent with the condition $(\Delta^{(Q)})^* = \Delta^{(-Q)}$.

For an n -dimensional representation, the ladder operator τ^+ satisfies

$$\tau^+ |e_k^{(n)}\rangle = \begin{cases} -\sqrt{(j-k)(j+k+1)} |e_{k+1}^{(n)}\rangle, & k \geq 0; \\ \sqrt{(j-k)(j+k+1)} |e_{k+1}^{(n)}\rangle, & k < 0. \end{cases} \quad (7)$$

Here $j = (n-1)/2$, and $k = -j, -j+1, \dots, j-1, j$. For $n = 2j+1 = 7$, τ^\pm can be explicitly expressed as

$$\tau^+ = \begin{pmatrix} 0 & -\sqrt{6} & & & & & \\ & 0 & -\sqrt{10} & & & & \\ & & 0 & -\sqrt{12} & & & \\ & & & 0 & \sqrt{12} & & \\ & & & & 0 & \sqrt{10} & \\ & & & & & 0 & \sqrt{6} \\ & & & & & & 0 \end{pmatrix}, \quad \tau^- = (\tau^+)^T. \quad (8)$$

With these matrices, the kinetic term and the couplings to the gauge fields of each component can be explicitly written down as

$$\begin{aligned}
\mathcal{L}_1 &= (D_\mu \Phi)^\dagger D^\mu \Phi \\
&= \frac{1}{2}(\partial_\mu \Delta^{(0)})^2 + \sum_{Q=1}^3 (\partial_\mu \Delta^{(Q)})(\partial^\mu \Delta^{(-Q)}) + \sum_{Q=1}^3 (QeA^\mu + Qg_2 c_W Z^\mu) \Delta^{(-Q)} i \overleftrightarrow{\partial}_\mu \Delta^{(Q)} \\
&\quad - g_2 W^{+, \mu} (\sqrt{3} \Delta^{(-3)} i \overleftrightarrow{\partial}_\mu \Delta^{(2)} + \sqrt{5} \Delta^{(-2)} i \overleftrightarrow{\partial}_\mu \Delta^{(1)} + \sqrt{6} \Delta^{(-1)} i \overleftrightarrow{\partial}_\mu \Delta^{(0)}) \\
&\quad - g_2 W^{-, \mu} (\sqrt{3} \Delta^{(-2)} i \overleftrightarrow{\partial}_\mu \Delta^{(3)} + \sqrt{5} \Delta^{(-1)} i \overleftrightarrow{\partial}_\mu \Delta^{(2)} + \sqrt{6} \Delta^{(0)} i \overleftrightarrow{\partial}_\mu \Delta^{(1)}) \\
&\quad + (e^2 A_\mu A^\mu + g_2^2 c_W^2 Z_\mu Z^\mu + 2eg_2 c_W A_\mu Z^\mu) \sum_{Q=1}^3 Q^2 \Delta^{(Q)} \Delta^{(-Q)} \\
&\quad + g_2^2 W_\mu^+ W^{-, \mu} [6(\Delta^{(0)})^2 + 11\Delta^{(1)}\Delta^{(-1)} + 8\Delta^{(2)}\Delta^{(-2)} + 3\Delta^{(3)}\Delta^{(-3)}] \\
&\quad - g_2^2 \{ W_\mu^+ (s_W A^\mu + c_W Z^\mu) (\sqrt{6}\Delta^{(0)}\Delta^{(-1)} + 3\sqrt{5}\Delta^{(1)}\Delta^{(-2)} + 5\sqrt{3}\Delta^{(2)}\Delta^{(-3)}) \\
&\quad + W_\mu^+ W^{+, \mu} [3(\Delta^{(-1)})^2 - \sqrt{30}\Delta^{(0)}\Delta^{(-2)} - \sqrt{15}\Delta^{(1)}\Delta^{(-3)}] + \text{h.c.} \}, \tag{9}
\end{aligned}$$

where $\overleftrightarrow{\partial}_\mu$ is defined as $F \overleftrightarrow{\partial}_\mu G = F \partial_\mu G - G \partial_\mu F$.

In this model, the potential is not only constructed by the Higgs doublet H , but also constructed by the septuplet Φ . Since Φ is real, the operator $\Phi^\dagger \tau^a \Phi$ vanishes, but a term as $(\Phi^\dagger T^a T^b \Phi)^2$ is allowed, and the general form of the potential is

$$\begin{aligned}
V &= \mu^2 H^\dagger H + m^2 \Phi^\dagger \Phi + \lambda(H^\dagger H)^2 + \lambda_2(\Phi^\dagger \Phi)^2 \\
&\quad + \lambda_3(H^\dagger H)(\Phi^\dagger \Phi) + \frac{\lambda_4}{48}(\Phi^\dagger T^a T^b \Phi)^2. \tag{10}
\end{aligned}$$

Comparing with the SM, there are three more couplings λ_2 , λ_3 , and λ_4 , and one more mass parameter m . Note that the last term in (10) can be separated from the traceless part (with respect to the indices a, b) as follows

$$\Phi^\dagger T^a T^b \Phi = \frac{1}{2} \Phi^\dagger \{T^a, T^b\} \Phi = \Phi^\dagger \left(\frac{1}{2} \{T^a, T^b\} - 4\delta^{ab} \right) \Phi + 4\delta^{ab} \Phi^\dagger \Phi. \tag{11}$$

where we have used $\Phi^\dagger T^a \Phi = 0$ and $T^a T^a = C_2(j)\mathbf{1} = j(j+1)\mathbf{1}$ with $j = 3$. Define $(S^{ab})_{ij} = \frac{1}{2} \{T^a, T^b\}_{ij} - 4\delta^{ab} \delta_{ij}$, and $(\Phi^\dagger T^a T^b \Phi)^2$ can be rewritten as a sum of two quadratic terms:

$$(\Phi^\dagger T^a T^b \Phi)^2 = (\Phi^\dagger S^{ab} \Phi)^2 + 48(\Phi^\dagger \Phi)^2. \tag{12}$$

Thus the potential can be expressed as

$$\begin{aligned}
V &= \mu^2 H^\dagger H + m^2 \Phi^\dagger \Phi + \lambda(H^\dagger H)^2 + (\lambda_2 + \lambda_4)(\Phi^\dagger \Phi)^2 \\
&\quad + \lambda_3(H^\dagger H)(\Phi^\dagger \Phi) + \frac{\lambda_4}{48}(\Phi^\dagger S^{ab} \Phi)^2. \tag{13}
\end{aligned}$$

We assume that the vacuum expectation value (VEV) of the Higgs field is nonzero but the VEV of Φ remains zero. Then the minimization condition implies that $\mu^2 < 0$ and $m^2 - \lambda_3\mu^2/(2\lambda) \geq 0$. As in the SM, the VEV of the Higgs doublet is $\langle H \rangle = (0, v/\sqrt{2})^T$, where $v \equiv \sqrt{-\mu^2/\lambda} = 246.22$ GeV.

After the Higgs field acquires a VEV, the potential term $\lambda_3(H^\dagger H)(\Phi^\dagger \Phi)$ contributes to the masses of all components of Φ . Even so, they are totally degenerate at the tree level with a value of m_0 , which satisfies

$$m_0^2 = m^2 + \frac{\lambda_3 v^2}{2}. \quad (14)$$

Mass splittings among the components are induced by loop corrections involving gauge bosons, and the charged components are slightly heavier than the neutral component. For $m_0 \gg m_Z$, the mass splitting between $\Delta^{(Q)}$ and $\Delta^{(0)}$ is [1]

$$m_Q - m_0 = Q^2 \Delta m, \quad (15)$$

where $\Delta m = \alpha_2 m_W \sin^2(\theta_W/2) \simeq 167$ MeV. For $m_0 \sim \mathcal{O}(\text{TeV})$, these splittings are very tiny and we can still regard the components degenerate.

2.2 Several relevant phenomenologies

2.2.1 DM phenomenologies

The septuplet mass threshold affects the cosmological DM relic abundance. In the following, we will quickly review the relic abundance calculation and obtain the mass threshold favored by observation. As discussed in Ref. [4], the thermal DM relic abundance for a real scalar MDM model can be approximately expressed as

$$\Omega_{\text{DM}} h^2 \simeq \frac{1.07 \times 10^9 \text{ GeV}^{-1}}{J(x_F) \sqrt{g_*} M_{\text{Pl}}} \quad \text{with} \quad J(x_F) = \int_{x_F}^{\infty} \frac{\langle \sigma_{\text{eff}} v \rangle}{x^2} dx, \quad (16)$$

where M_{Pl} is the Planck mass and g_* is the total number of effectively relativistic degrees of freedom. The effective thermally averaged annihilation cross section is defined by

$$\langle \sigma_{\text{eff}} v \rangle \equiv \sum_{QQ'} \langle \sigma_{QQ'} v \rangle \frac{n_Q^{\text{eq}} n_{Q'}^{\text{eq}}}{(n^{\text{eq}})^2}, \quad (17)$$

where $\sigma_{QQ'}$ is the annihilation cross section between the multiplet components $\Delta^{(Q)}$ and $\Delta^{(Q')}$. $n_Q^{\text{eq}} = (m_Q T/2\pi)^{3/2} \exp(-m_Q/T)$ is the thermal equilibrium density of $\Delta^{(Q)}$, and $n^{\text{eq}} \equiv \sum_Q n_Q^{\text{eq}}$. By such a definition of $\langle \sigma_{\text{eff}} v \rangle$, we take into account the coannihilation effect among the multiplet components. x_F is the freeze-out parameter that can be obtained by solving the equation

$$x_F = \ln \frac{0.0038 M_{\text{Pl}} g_{\text{eff}} m_0 \langle \sigma_{\text{eff}} v \rangle}{\sqrt{g_*} x_F}, \quad (18)$$

where the effective number of degrees of freedom $g_{\text{eff}} = \sum_Q n_Q^{\text{eq}}/n_0^{\text{eq}}$.

Neglecting the mass splittings among the multiplet components, we have $n_Q^{\text{eq}} \simeq n_{Q'}^{\text{eq}}$ for any $\Delta^{(Q)}$ and $\Delta^{(Q')}$, and hence $\langle\sigma_{\text{eff}}v\rangle \simeq \sum_{QQ'} \langle\sigma_{QQ'}v\rangle/n^2$ and $g_{\text{eff}} \simeq n$. Since the s -wave annihilations into gauge and Higgs bosons are dominant, for $m_0 \gg m_h$ we have

$$\langle\sigma_{\text{eff}}v\rangle \simeq \frac{(n^2 - 1)(n^2 - 3)}{n} \frac{\pi\alpha_2^2}{8m_0^2} + \frac{1}{n} \frac{\lambda_3^2}{16\pi m_0^2}, \quad (19)$$

where $\alpha_2 \equiv g_2^2/(4\pi)$. For a heavier DM particle, $\langle\sigma_{\text{eff}}v\rangle$ would be smaller and lead to a larger abundance. For the septuplet model, $n = 7$, and we take $x_F \simeq 25$ and $\sqrt{g_*} \simeq 10.33$ for $T \sim \mathcal{O}(\text{TeV})$, and calculate the relic abundance.

Fixing the relic abundance to its observed value $\Omega_{\text{DM}}h^2 = 0.1196 \pm 0.0031$ [19], we can constrain the parameters m_0 and λ_3 . In Fig. 1, the 1σ favored region is denoted by a purple strip in the λ_3 - m_0 plane. In this strip, m_0 increases as $|\lambda_3|$ increases. For $\lambda_3 = 0$, m_0 achieves its threshold mass, $\simeq 8.8$ TeV. The calculation above has not included the SE effect, which can increase annihilation cross sections and hence reduce the relic abundance for fixed m_0 and λ_3 . As suggested in Refs. [2, 4], the SE factor at the freeze-out epoch is almost a constant, and we can simply increase $\langle\sigma_{\text{eff}}v\rangle$ by a scale factor $\simeq 8$ to take this effect into account in the septuplet model. The dashed purple line in Fig. 1 corresponds to the observed relic abundance including the SE effect. In this case, the threshold mass is about 25 TeV.

A more accurate treatment for the DM relic abundance in real scalar MDM models can be found in Ref. [4], and gives a threshold septuplet mass of 7.9 (22.4) TeV without (with) the SE effect using the WMAP data. These results are about 10% smaller than our approximate results here. Nonetheless, these discrepancies would not essentially change the following analysis on the vacuum stability and the perturbativity of couplings.

We also briefly comment on the direct and indirect detection bounds on this DM candidate. At tree level, only the SM Higgs boson mediates the DM-nucleon scattering, but the rate is greatly suppressed by the heavy DM mass squared and thus is negligible as long as λ_3 is not very large (later we will see that this is true after taking into account vacuum stability). However, at loop level there is a contribution that is not so suppressed [1]:

$$\sigma_{\text{DM-N}}^{(1)} = \frac{36\pi\alpha_2^4 f_N^2 m_N^4}{m_W^2} \left(\frac{1}{m_W^2} + \frac{1}{m_h^2} \right)^2. \quad (20)$$

where $f_N \simeq 0.3$ is the nucleonic form factor [20] and $m_N \simeq 1$ GeV is the nucleon mass. This cross section, independent of m_0 , has a value of $\simeq 4 \times 10^{-44}$ cm². Therefore, the 90% C.L. exclusion limit from LUX [21] can exclude the range of $m_0 \lesssim 3.3$ TeV, as shown by the grey region in Fig. 1. For indirect searches, the

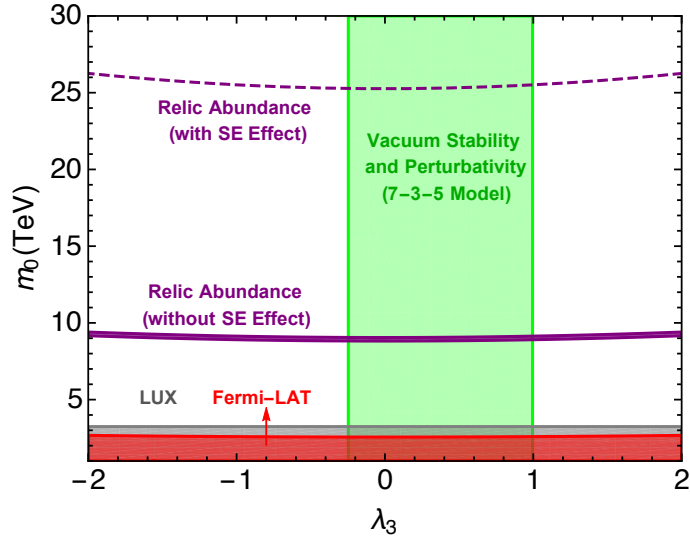


Figure 1: Regions favored by the observed DM relic abundance in the λ_3 - m_0 plane. The purple (dashed) strip corresponds to the 1σ range of the relic abundance measured by the Planck experiment for the case without (with) the Sommerfeld enhancement effect. The green band is the region satisfying the vacuum stability and the perturbativity conditions in the 7-3-5 model. The grey and red regions are excluded by the LUX and Fermi-LAT results at 90% and 95% C.L., respectively.

most promising annihilation channel is the W^+W^- channel, which has a cross section $\sim 9g_2^4/\pi m_{\text{DM}}^2$ ⁴. The Fermi-LAT limit [23] excludes the range of $m_0 \gtrsim 2.5$ TeV for $|\lambda_3| \lesssim 2$, as shown by the red region in Fig. 1.

2.2.2 Vacuum stability

The VS conditions can be obtained by means of the copositive criteria [24]. However, it is not quite straightforward to obtain these conditions in the septuplet model. The obstacle is from the quartic term $\mathcal{Q}_1 \equiv (\Phi^\dagger S^{ab} \Phi)^2$, which, unlike the conventional term $\mathcal{Q}_0 \equiv (\Phi^\dagger \Phi)^2$, yields non-universal (even in sign) quartic terms for different components. To see this, we explicitly expand \mathcal{Q}_1 in components as

$$\begin{aligned} \frac{\mathcal{Q}_1}{48} = & \frac{1}{8}(\Delta^{(0)})^4 + \frac{21}{32}|\Delta^{(1)}|^4 + \frac{25}{32}|\Delta^{(3)}|^4 \\ & + \frac{1}{2}|\Delta^{(1)}|^2(\Delta^{(0)})^2 + \frac{5}{4}|\Delta^{(2)}|^2(\Delta^{(0)})^2 - \frac{5}{8}|\Delta^{(3)}|^2(\Delta^{(0)})^2 \\ & + \frac{15}{16}|\Delta^{(1)}|^2|\Delta^{(2)}|^2 - \frac{5}{16}|\Delta^{(1)}|^2|\Delta^{(3)}|^2 + \frac{25}{16}|\Delta^{(2)}|^2|\Delta^{(3)}|^2 \end{aligned}$$

⁴The ZZ/hh channels produce similar gamma-ray spectra to that from the WW channel [22], but the cross section $\simeq \lambda_3^2/64\pi m_{\text{DM}}^2$, depending on λ_3 .

$$\begin{aligned}
& -\frac{\sqrt{15}}{8\sqrt{2}}(\Delta^{(-2)}(\Delta^{(1)})^2\Delta^{(0)} + \Delta^{(2)}(\Delta^{(-1)})^2\Delta^{(0)}) \\
& -\frac{\sqrt{15}}{8}(\Delta^{(-3)}(\Delta^{(1)})^3 + (\Delta^{(-1)})^3\Delta^{(3)}) \\
& +\frac{5}{16}\sqrt{15}(\Delta^{(-3)}\Delta^{(-1)}(\Delta^{(2)})^2 + (\Delta^{(-2)})^2\Delta^{(1)}\Delta^{(3)}) \\
& +\frac{15}{8\sqrt{2}}(\Delta^{(-3)}\Delta^{(1)}\Delta^{(2)}\Delta^{(0)} + \Delta^{(-2)}\Delta^{(-1)}\Delta^{(3)}\Delta^{(0)}). \tag{21}
\end{aligned}$$

Vacuum stability concerns the behavior of the potential as the field values go to infinity. This allows us to reduce \mathcal{Q}_1 . The key observation is that the ratio $\mathcal{Q}_1/(48\mathcal{Q}_0)$ reaches its maximum $25/32$ and minimum 0 when Φ goes to infinity along the $\Delta^{(3)}$ and $\Delta^{(2)}$ directions, respectively. Therefore, we can parametrize $\mathcal{Q}_1/48$ as $25\rho\mathcal{Q}_0/32$ with $0 \leq \rho \leq 1$. Then the potential becomes

$$\begin{aligned}
V = & \mu^2 H^\dagger H + m^2 \Phi^\dagger \Phi + \lambda(H^\dagger H)^2 + \lambda_3(H^\dagger H)(\Phi^\dagger \Phi) \\
& + \left[(\lambda_2 + \lambda_4) + \frac{25}{32}\rho\lambda_4 \right] (\Phi^\dagger \Phi)^2. \tag{22}
\end{aligned}$$

Now we can use the copositive criteria to get the VS conditions, which depend on the sign of λ_4 . For $\lambda_4 \geq 0$, the bottom of the potential is achieved when $\rho = 0$ and the VS conditions are

$$\begin{cases} \lambda \geq 0, \\ \lambda_2 + \lambda_4 \geq 0, \\ \lambda_3 + 2\sqrt{\lambda(\lambda_2 + \lambda_4)} \geq 0. \end{cases} \tag{23}$$

While for $\lambda_4 < 0$ the bottom is achieved when $\rho = 1$, and the VS conditions turn out to be

$$\begin{cases} \lambda \geq 0, \\ \lambda_2 + \frac{57}{32}\lambda_4 \geq 0, \\ \lambda_3 + 2\sqrt{\lambda(\lambda_2 + \frac{57}{32}\lambda_4)} \geq 0. \end{cases} \tag{24}$$

Note that λ can never be negative.

3 Confronting perturbativity

In the framework of quantum field theory, perturbativity is important to guarantee the self-consistency of perturbative calculations. The breakdown of perturbativity at some scale, known as the Landau pole scale Λ_{LP} , implies that a new theory should appear hereafter. Perturbativity imposes a strong bound on models. In this section we firstly show that the minimal model suffers the Landau pole problem around 10^8 GeV. Then we attempt to push it up to 10^{14} GeV by introducing Yukawa couplings to the septuplet.

3.1 Perturbativity bound on the septuplet model

In the real scalar septuplet MDM model, there are mainly two modifications that may endanger perturbativity. One is a large positive contribution to the beta function of g_2 from the 7-dimensional representation. It drives g_2 towards the Landau pole more quickly. The other one is the focus of this paper, the fast increase of MDM self-couplings owing to their impressively large beta functions. Explicitly, the one-loop formulas can be calculated using the general formulas presented in Ref. [25] (or instead formulas up to two-loop are available using the code `PyR@TE` [26]),

$$\beta_{g_1} = \beta_{g_1}^{\text{SM}}, \quad \beta_{g_2} = \beta_{g_2}^{\text{SM}} + \frac{1}{16\pi^2} \frac{14}{3} g_2^3, \quad \beta_{g_3} = \beta_{g_3}^{\text{SM}}, \quad \beta_{y_t} = \beta_{y_t}^{\text{SM}}, \quad (25)$$

$$\beta_\lambda = \beta_\lambda^{\text{SM}} + \frac{1}{16\pi^2} \frac{7}{2} \lambda_3^2, \quad \beta_{\lambda_2} = \frac{1}{16\pi^2} [30\lambda_2^2 + 2\lambda_3^2 + \frac{45}{2} \lambda_4^2 + 51\lambda_2\lambda_4 - 144g_2^2\lambda_2], \quad (26)$$

$$\beta_{\lambda_3} = \frac{1}{16\pi^2} \left[12\lambda\lambda_3 + 18\lambda_2\lambda_3 + 4\lambda_3^2 + \frac{51}{2} \lambda_3\lambda_4 + 36g_2^4 - \lambda_3 \left(\frac{153}{2} g_2^2 + \frac{9}{10} g_1^2 - 6y_t^2 \right) \right], \quad (27)$$

$$\beta_{\lambda_4} = \frac{1}{16\pi^2} \left[288g_2^4 + \frac{255}{8} \lambda_4^2 + 24\lambda_2\lambda_4 - 144g_2^2\lambda_4 \right]. \quad (28)$$

Our results coincide with those obtained in Ref. [17] except for the $\lambda_3\lambda_4$ -term in β_{λ_3} , which seems to be overlooked in that paper. But it does not affect perturbativity much. Additionally, we have rescaled the quartic couplings λ_4 by a factor 1/48 and thus the numerical coefficients differ much from theirs. The beta functions in the SM are

$$\beta_{g_1}^{\text{SM}} = \frac{1}{16\pi^2} \frac{41}{10} g_1^3, \quad \beta_{g_2}^{\text{SM}} = \frac{1}{16\pi^2} \left(-\frac{19}{6} \right) g_2^3, \quad \beta_{g_3}^{\text{SM}} = \frac{1}{16\pi^2} (-7) g_3^3, \quad (29)$$

$$\beta_{y_t}^{\text{SM}} = \frac{1}{16\pi^2} y_t \left(\frac{9}{2} y_t^2 - \frac{9}{4} g_2^2 - \frac{17}{20} g_1^2 - 8g_3^2 \right), \quad (30)$$

$$\beta_\lambda^{\text{SM}} = \frac{1}{16\pi^2} \left\{ 24\lambda^2 - 6y_t^4 + \frac{3}{8} \left[2g_2^4 + \left(g_2^2 + \frac{3}{5} g_1^2 \right)^2 \right] + \lambda \left(-9g_2^2 - \frac{9}{5} g_1^2 + 12y_t^2 \right) \right\}. \quad (31)$$

From the weak scale to the septuplet threshold, couplings are evolving according to these functions.

Before heading towards the numerical study, we briefly introduce some numerical conventions. The $\overline{\text{MS}}$ values of gauge couplings at the electroweak scale are given by [27]

$$\alpha_s(m_Z) = \frac{g_s(m_Z)^2}{4\pi} = 0.1184 \pm 0.0007, \quad (32)$$

$$\alpha(m_Z) = \frac{[g_2(m_Z)s_W(m_Z)]^2}{4\pi} = \frac{1}{127.926}, \quad (33)$$

$$s_W^2 = \sin^2 \theta_W(m_Z) = 0.2312. \quad (34)$$

The measured values of y_t and λ are actually determined from the observed masses of the top quark and the Higgs boson, m_t and m_h , respectively. Therefore, we need to derive the $\overline{\text{MS}}$ values $y_t(m_Z)$ and $\lambda(m_Z)$ at the electroweak scale by the matching conditions [28]

$$y_t(\mu_0) = \frac{\sqrt{2}m_t}{v}[1 + \delta_t(\mu_0)], \quad \lambda(\mu_0) = \frac{m_h^2}{2v^2}[1 + \delta_h(\mu_0)], \quad (35)$$

with setting $\mu_0 = m_Z$. The related functions are

$$\delta_t(\mu_0) = \left(-\frac{4\alpha_s}{4\pi} - \frac{4}{3}\frac{\alpha}{4\pi} + \frac{9}{4}\frac{m_t^2}{16\pi^2 v^2} \right) \ln \frac{\mu_0^2}{m_t^2} + c_t, \quad (36)$$

$$\delta_h(\mu_0) = \frac{2v^2}{m_h^2} \frac{1}{32\pi^2 v^4} [h_0(\mu_0) + m_h^2 h_1(\mu_0) + m_h^4 h_2(\mu_0)], \quad (37)$$

$$h_0(\mu_0) = -24m_t^4 \ln \frac{\mu_0^2}{m_t^2} + 6m_Z^4 \ln \frac{\mu_0^2}{m_Z^2} + 12m_W^4 \ln \frac{\mu_0^2}{m_W^2} + c_0, \quad (38)$$

$$h_1(\mu_0) = 12m_t^2 \ln \frac{\mu_0^2}{m_t^2} - 6m_Z^2 \ln \frac{\mu_0^2}{m_Z^2} - 12m_W^2 \ln \frac{\mu_0^2}{m_W^2} + c_1, \quad (39)$$

$$h_2(\mu_0) = \frac{9}{2} \ln \frac{\mu_0^2}{m_h^2} + \frac{1}{2} \ln \frac{\mu_0^2}{m_Z^2} + \ln \frac{\mu_0^2}{m_W^2} + c_2. \quad (40)$$

The constants c_0 , c_1 , and c_2 are independent of the scale μ_0 , and their contributions to δ_h are less than 0.02. The constant c_t lies in the range of $-0.052 \leq c_t \leq -0.042$. Thus we neglect c_0 , c_1 and c_2 and take $c_t = -0.052$ in the calculation. Choosing other values for c_t would not essentially change our results.

It is illustrative to make some analysis of the RGEs (25)–(28). An analytical solution is impossible, despite an approximate solution treating g_2 as constant during running [17]⁵. Even if the initial values of λ_2 and λ_4 are both zero, their Landau poles appear not very far from the septuplet threshold. The presence of the λ_4 -term is crucial. The large positive contributions to β_{λ_4} from the g_2^4 - and λ_4^2 -terms drive λ_4 increasing quickly. Then the terms involving λ_4 in β_{λ_2} (with large positive coefficients) push λ_2 towards the Landau pole. As a matter of fact, λ_2 hits the Landau pole first. Given the septuplet MDM threshold $\Lambda = 8.8$ TeV or 25 TeV and initial values of $\lambda_2(\Lambda) = \lambda_4(\Lambda) = 0$, we have $\Lambda_{\text{LP}} \sim 10^8 - 10^9$ GeV. Here and henceforth, we set the septuplet threshold Λ to be 25 TeV, and the evolution of λ_2 and λ_4 are indicated by the solid lines in Fig. 2. This is consistent with the result

⁵The authors in Ref. [17] gave an estimation of the Landau pole as $\Lambda_{\text{LP}} = 1.0 \times 10^6 \left(\frac{m}{100 \text{ GeV}} \right)^{1.13}$.

in Ref. [17]. If the VS conditions were not imposed, it would be able to obtain a slightly higher $\Lambda_{\text{LP}} \sim 10^{10}$ GeV by arranging a cancellation between the $\lambda_4\lambda_2$ -term and λ_2^2 -term in β_{λ_2} . For instance, This can be achieved if we set $\lambda_2(\Lambda) = 2$ and $\lambda_4(\Lambda) = -2$, as demonstrated in the left panel of Fig. 2. On the other hand, if $\lambda_2(\Lambda) < 0$ and $\lambda_4(\Lambda) > 0$, the situation would be even worse, as shown in the right panel of Fig. 2.

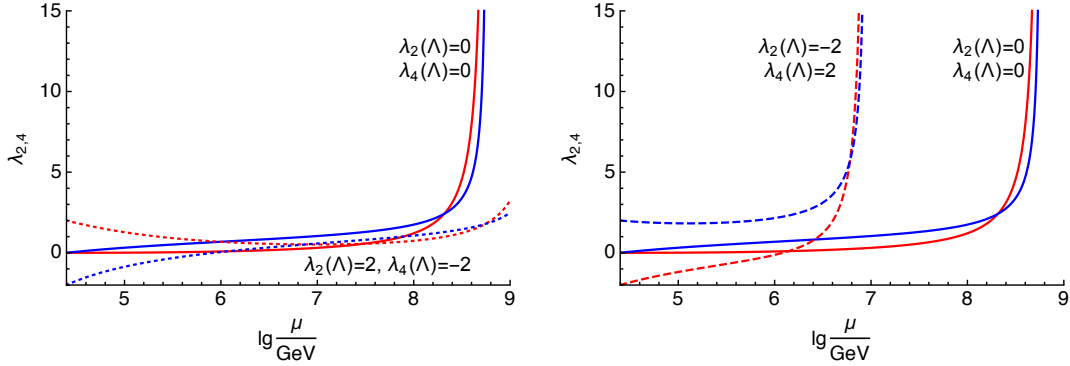


Figure 2: The evolution of λ_2 (red lines) and λ_4 (blue lines) in the septuplet MDM model.

3.2 Push up the Landau pole scale in the 7-3-5 model

It is potential to push up the LP scale by introducing Yukawa couplings to the septuplet. This is inspired by the beta function structure of the Higgs self-coupling λ . It receives a large negative contribution from the top quark Yukawa coupling, which incurs the metastable problem of the electroweak vacuum at high scales. We will firstly present the 7-3-5 model, which is an extension to the septuplet model, and then analyze its implication to the Landau pole problem.

3.2.1 The 7-3-5 model

In order to construct Yukawa couplings to the septuplet, extra fermions should be introduced. Three minimal ways are available: $(1, 0) \oplus (7, 0)$, $(3, 0) \oplus (5, 0)$ and $(4, 0) \oplus (4, 0)$. The first and second options have potential of explaining the tiny neutrino masses via the type-I and type-III seesaw mechanisms⁶, respectively. However, we find that the first option is not as good as the second one due to a fairly large contribution to β_{g_2} from the fermionic septuplet. On the other hand, in the last option, if the two $(4, 0)$ fermions belong to the same chiral field (namely

⁶There are some models with quintuplet fermion and septuplet scalar for generating neutrino masses at loop level [29–31].

being Majorana fermions), it would lead to the problem of Witten global anomaly [32, 33]. Even worse, the Majorana mass term violates the accidental Z_2 symmetry of the septuplet and thus leads to the septuplet MDM radiatively decay into a pair of gauge bosons. A (4, 0) Dirac fermion avoids the Witten global anomaly, but it similarly endangers the stability of MDM at loop level. Therefore, in this work we concentrate on the $(3, 0) \oplus (5, 0)$ case, and the resulting model is dubbed as the 7-3-5 model.

In order to write down the Yukawa interaction terms, it is more convenient to use the tensor notation rather than the vector notation adopted above. More details about the tensor notation can be found in Ref. [29]. The dictionary from the latter to the former notation reads

$$\Phi = \frac{1}{\sqrt{2}} \begin{pmatrix} \Delta^{(3)} \\ \Delta^{(2)} \\ \Delta^{(1)} \\ \Delta^{(0)} \\ \Delta^{(-1)} \\ \Delta^{(-2)} \\ \Delta^{(-3)} \end{pmatrix} = \frac{1}{\sqrt{2}} \begin{pmatrix} \Phi_{111111} \\ \sqrt{6}\Phi_{111112} \\ \sqrt{15}\Phi_{111122} \\ \sqrt{20}\Phi_{111222} \\ -\sqrt{15}\Phi_{112222} \\ \sqrt{6}\Phi_{122222} \\ -\Phi_{222222} \end{pmatrix}, \quad (41)$$

$$\Psi_L = \begin{pmatrix} \Psi_{+2,L} \\ \Psi_{+1,L} \\ \Psi_{0,L} \\ \Psi_{-1,L} \\ \Psi_{-2,L} \end{pmatrix} = \begin{pmatrix} \Psi_{1111,L} \\ 2\Psi_{1112,L} \\ \sqrt{6}\Psi_{1122,L} \\ -2\Psi_{1222,L} \\ \Psi_{2222,L} \end{pmatrix}, \quad \Sigma_R = \begin{pmatrix} \Sigma_{+1,R} \\ \Sigma_{0,R} \\ \Sigma_{-1,R} \end{pmatrix} = \begin{pmatrix} \Sigma_{11,R} \\ \sqrt{2}\Sigma_{12,R} \\ -\Sigma_{22,R} \end{pmatrix}. \quad (42)$$

Here we have assigned the left and right chiralities to the quintuplet and triplet, respectively. At renormalizable level the most generic Yukawa interactions can be written down as

$$\mathcal{L}_{\text{yuk}} = -\sqrt{15}y\Phi_{ijklmn}\overline{\Psi}_L^{ijkl}\Sigma_{R,m'n'}\varepsilon^{mm'}\varepsilon^{nn'} \\ -(y_\Sigma)_{ab}\overline{l}_{a,L}^i(\Sigma_{b,R})_{ij}H_k\varepsilon^{jk} + \text{h.c.}, \quad (43)$$

where $i, j, k, l, m, n = 1, 2$ are $SU(2)_L$ tensor indices and symmetric for Φ , Ψ , and Σ . a and b are family indices and for the sake of realistic neutrino mixing at least two triplets are required. Terms in the second line, along with Majorana mass terms for the fermions, constitute the type-III seesaw mechanism. The Yukawa couplings y_Σ are irrelevantly small. Note that the 7-dimensional representation from the decomposition $5 \times 5 = 1_S + 3_A + 5_S + 7_A + 9_S$ is antisymmetric, thus the coupling $\Phi\Psi\Psi$ vanishes. In the vector notation, Eq. (43) gives the Yukawa couplings of the septuplet as

$$\mathcal{L}_{\text{yuk}} = \frac{y}{\sqrt{2}}\{[\Delta^{(0)}\sqrt{3}\overline{\Psi}_{-1}\Sigma_{-1} + \Delta^{(-1)}(-\sqrt{6}\overline{\Psi}_0\Sigma_{+1} - 2\sqrt{2}\overline{\Psi}_{-1}\Sigma_0 + \overline{\Psi}_{-2}\Sigma_{-1})$$

$$\begin{aligned}
& + \Delta^{(-2)}(-\sqrt{10}\overline{\Psi}_{-1}\Sigma_{+1} - \sqrt{5}\overline{\Psi}_{-2}\Sigma_0) - \sqrt{15}\Delta^{(-3)}\overline{\Psi}_{-2}\Sigma_{+1} + \text{h.c.}] \\
& - 3\Delta^{(0)}\overline{\Psi}_0\Sigma_0\}.
\end{aligned} \tag{44}$$

Where $\Psi_{-Q} = \Psi_{-Q,L} + (\Psi_{+Q,L})^c$ and $\Sigma_{-Q} = \Sigma_{-Q,L} + (\Sigma_{+Q,L})^c$. The gauge couplings of the fermions are

$$\begin{aligned}
\mathcal{L}_{\text{gauge}} = & g_2[(\sqrt{3}\overline{\Psi}_0\gamma^\mu\Psi_{-1} + \sqrt{2}\overline{\Psi}_{-1}\gamma^\mu\Psi_{-2})W_\mu^+ + \overline{\Sigma}_0\gamma^\mu\Sigma_{-1}W_\mu^+ + \text{h.c.}] \\
& + g_2\left(\sum_{Q=1}^2 Q\overline{\Psi}_Q\gamma^\mu\Psi_Q + \overline{\Sigma}_{+1}\gamma^\mu\Sigma_{+1}\right)W_\mu^3.
\end{aligned} \tag{45}$$

The presence of the quintuplet and triplet further modifies the one-loop beta functions with the following extra terms:

$$\delta\beta_{g_2} = \frac{8g_2^3}{16\pi^2}, \tag{46}$$

$$\delta\beta_{\lambda_2} = \frac{1}{16\pi^2}(-54y^4 + 40y^2\lambda_2), \tag{47}$$

$$\delta\beta_{\lambda_3} = \frac{20y^2\lambda_3}{16\pi^2}, \tag{48}$$

$$\delta\beta_{\lambda_4} = \frac{1}{16\pi^2}(-96y^4 + 40y^2\lambda_4), \tag{49}$$

$$\beta_y = \frac{y}{16\pi^2}(25y^2 - 24g_2^2). \tag{50}$$

As expected, the Yukawa coupling y has negative contributions to β_{λ_2} and β_{λ_4} . Below we study how the LP scale can be substantially pushed up by this coupling.

3.2.2 How high can the Landau pole scale be?

Now we have two free parameters at hand. One is y ; the other one is M_{35} , the threshold above which the 7-3-5 Yukawa coupling becomes active. The mass scales of the quintuplet and triplet are set to be equal to M_{35} ⁷. In order to push up Λ_{LP} as high as possible, we find that M_{35} should not be far above the MDM mass scale, and moreover the initial value of $y(M_{35})$ should be fine-tuned. Thereby, the 7-3-5 model does not provide a quite satisfactory alleviation to the Landau pole problem.

First of all, the Landau pole of g_2 is of concern. As shown in Eq. (46), the beta function of g_2 receives large positive contributions from the quintuplet and triplet. Consequently, a low M_{35} would drive g_2 to the Landau pole quickly⁸. The explicit

⁷In practice, M_{35} can be identified as the heavier one. But the situation is actually worse since the lighter fermion just induces increase in g_2 from its mass to M_{35} .

⁸To maximize the Landau pole scale of g_2 , we assume a hierarchy between different triplet generations and only the lightest one is active at the low energy scales we concern.

solution is

$$\alpha_2^{-1}(\mu) = \alpha_2^{-1}(m_Z) - \frac{b_2^{\text{SM}}}{2\pi} \ln \frac{\Lambda}{m_Z} - \frac{b_2^{\text{sep}}}{2\pi} \ln \frac{M_{35}}{\Lambda} - \frac{b_2^{\text{tot}}}{2\pi} \ln \frac{\mu}{M_{35}}, \quad (51)$$

where $b_2^{\text{SM}} = -19/6$, $b_2^{\text{sep}} = 3/2$, and $b_2^{\text{tot}} = 19/2$. From it one can determine the Landau pole scale of g_2 :

$$\Lambda_{\text{LP}}^{(g_2)} = M_{35} \left(\frac{\Lambda}{M_{35}} \right)^{b_2^{\text{sep}}/b_2^{\text{tot}}} \exp \left[\frac{2\pi}{b_2^{\text{tot}}} \alpha_2^{-1}(\Lambda) \right]. \quad (52)$$

For example, if $M_{35} = 10^5$ GeV, we have $\Lambda_{\text{LP}}^{(g_2)} = 1.54 \times 10^{14}$ GeV, far below the Planck scale. Note that typically the non-perturbative scale is only slightly lower than Λ_{LP} , so we do not distinguish them in this paper.

One cannot rely on increasing M_{35} to lift $\Lambda_{\text{LP}}^{(g_2)}$. As our purpose is to push up the Landau pole scales of λ_2 and λ_4 , M_{35} is forced to be not far from the septuplet threshold Λ . Otherwise, λ_2 , perhaps as well as λ_4 , would quickly evolve to a sufficiently large value such that $y(M_{35}) \gg 1$ is needed to slow down the running of λ_2 and λ_4 . Moreover, y itself grows very fast and eventually diverges at $\Lambda_{\text{LP}}^{(y)}$, which could be much lower than $\Lambda_{\text{LP}}^{(g_2)}$. We can see this from the explicit expression of $y(t)$, where $t \equiv \ln(\mu/M_{35})$ denotes the logarithm of the energy scale. In practice, RGE (50) can be analytically solved:

$$y^2(t) = \frac{(24 + b_2)g_2^2(0)}{F_0[g_2(t)/g_2(0)]^{48/b_2} + 25[g_2(t)/g_2(0)]^{-2}}, \quad (53)$$

with $F_0 \equiv (24 + b_2)g_2^2(0)/y^2(0) - 25$ and $b_2 = b_2^{\text{tot}} = 19/2$.

As long as we have a large $y(0)$ such that $F_0 < 0$, $y(t)$ will meet the Landau pole as $g_2(t)$ evolves to the value

$$g_2^2(t_{\text{LP}}^{(y)}) \simeq g_2^2(0) \left(\frac{25}{|F_0|} \right)^{b_2/(24+b_2)} = g_2^2(0) \left[1 - \frac{(24 + b_2)g_2^2(0)}{25y^2(0)} \right]^{-b_2/(24+b_2)}. \quad (54)$$

Based on this equation, it is straightforward to derive an expression for $\Lambda_{\text{LP}}^{(y)}$:

$$\Lambda_{\text{LP}}^{(y)} = \frac{\Lambda_{\text{LP}}^{(g_2)}}{\exp \left[\frac{8\pi^2}{b_2 g_2^2(0)} \left(\frac{-F_0}{25} \right)^{b_2/(24+b_2)} \right]}. \quad (55)$$

Critical values that lead to $F_0 = 0$ and $\Lambda_{\text{LP}}^{(y)} = \Lambda_{\text{LP}}^{(g_2)}$ are $\pm y_c$, where

$$y_c \equiv \left(\frac{24 + b_2}{25} \right)^{1/2} g_2(0). \quad (56)$$

Thus $F_0 = 25[y_c^2/y^2(0) - 1]$. Since $\Lambda_{\text{LP}}^{(y)}$ is exponentially suppressed compared to $\Lambda_{\text{LP}}^{(g_2)}$, a small derivation of F_0 from zero will lead to a dramatically smaller $\Lambda_{\text{LP}}^{(y)}$, as shown in Fig. 3, where the labels on the lines are values of $y(0)$ in unit of y_c and $y(0) > y_c$ corresponds to $F_0 < 0$. In other words, in order to retain a high $\Lambda_{\text{LP}}^{(y)}$, $y(0)$ must be extremely close to $\pm y_c$. This raises a fine-tuning problem.

Unfortunately, this kind of fine-tuning is robust in any case. In the case of $F_0 > 0$, $y(t)$ no longer has a Landau pole but instead become asymptotic free as $g_2(t)$ approaches its Landau pole. Due to the large power $48/b_2 \approx 5.1$, $y(t)$ will quickly run to zero once the first term of the denominator in Eq. (53) dominates. We demonstrate this behavior for several $y(0)$ values in Fig. 3, where $y(0) < y_c$ corresponds to $F_0 > 0$. One can clearly see that $y(0)$ must be also sufficiently close to the critical value y_c , otherwise the Yukawa effect becomes negligible soon and the LP scales of λ_2 and λ_4 cannot be pushed up. Therefore, this case is not supposed to be better than the previous case. But it has an advantage that λ_2 and λ_4 are positive near their Landau poles. By contrast, in the $F_0 < 0$ case they run to large negative values near the Landau pole of $y(t)$. We can see these features in Fig. 4. We leave an analytical understanding of the Landau poles of λ_2 and λ_4 in the next subsection.

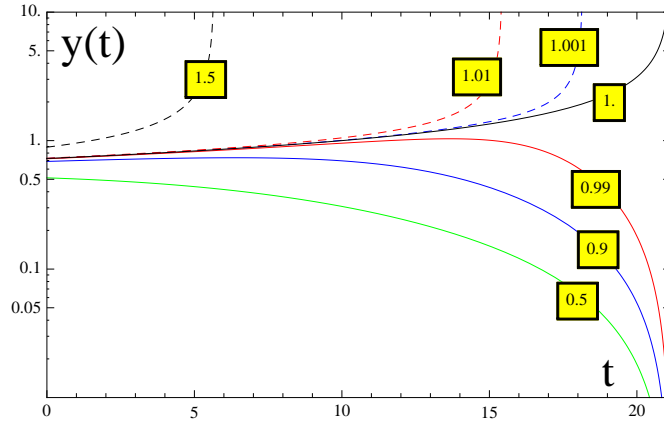


Figure 3: Running of $y(t)$ for different choices of $y(0)$, which is the labels on the lines in unit of y_c . The LP scale of g_2 is at the maximum of the t -axis. We have chosen $M_{35} = 10^{5.5}$ GeV, but the curves are not sensitive to this value.

From this analysis we can learn how to choose values of M_{35} that can lead to the highest LP scales. It should be chosen to guarantee a negative $\beta_{\lambda_2}(0) \sim -\mathcal{O}(0.01)$ such that the most intractable coupling λ_2 is tamed. Bear in mind that since $y(0)$ has been almost fixed around 0.7 by the condition $F_0 \approx 0$, there is a strong upper bound on M_{35} . In terms of our numerical investigation, the highest M_{35} is larger than the septuplet threshold Λ by about (typically slightly less than) 2 orders of

magnitude. For instance, for $m_{\text{DM}} = 22$ TeV, it is found that $M_{35} \approx 10^{5.7}$ GeV is required and the resulting maximal Landau pole scale is $\Lambda_{\text{LP}} \approx 10^{13}$ GeV if we tolerate $y(0) = 1.001y_c$; If we only tolerate $y(0) = 1.01y_c$, the maximal Landau pole is $\Lambda_{\text{LP}} \approx 10^{12}$ GeV with $M_{35} \approx 10^{6.1}$ GeV. We show the running in these two cases in Fig 4. For comparison, we also plot two cases with $F_0 > 0$: $y(0) = 0.99y_c$ with $M_{35} = 10^{5.5}$ GeV and $\Lambda_{\text{LP}} \approx 1.7 \times 10^{11}$ GeV; $y(0) = 0.999y_c$ with $M_{35} = 10^{5.6}$ GeV and $\Lambda_{\text{LP}} \approx 9.6 \times 10^{11}$ GeV.

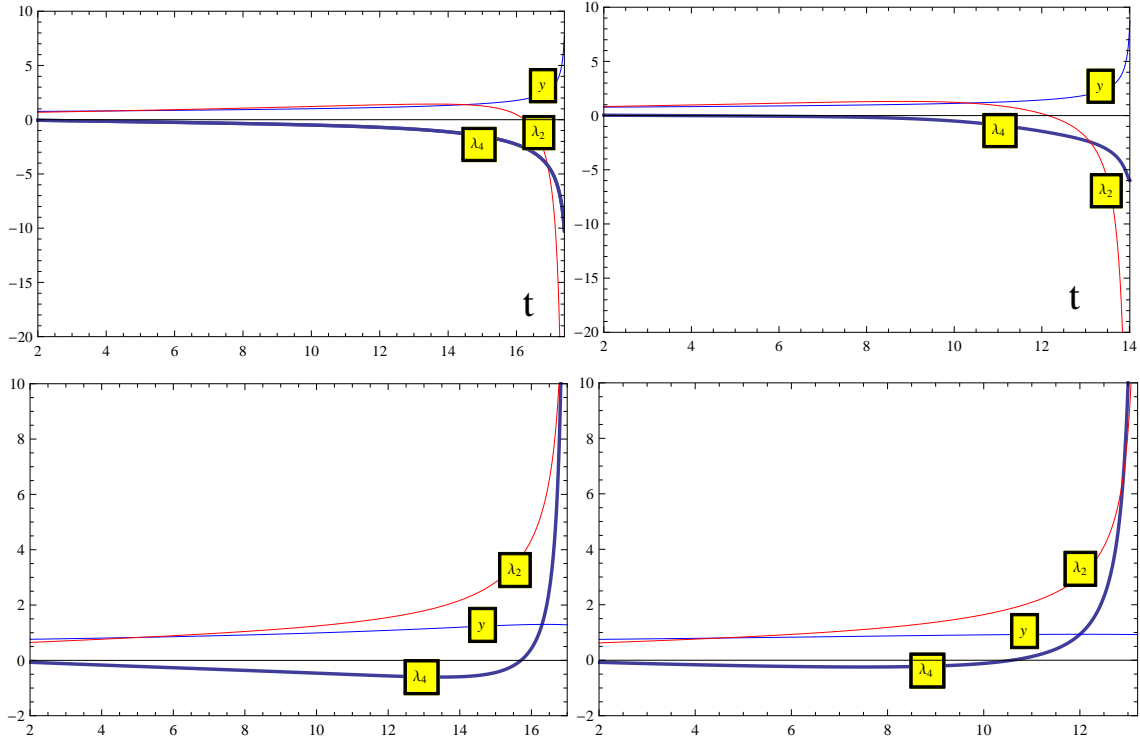


Figure 4: RGE running of couplings in four cases. Top left: $y(0) = 1.001y_c$ with $M_{35} = 10^{5.7}$ GeV; Top right: $y(0) = 1.01y_c$ with $M_{35} = 10^{6.1}$ GeV; Bottom left: $y(0) = 0.999y_c$ with $M_{35} = 10^{5.6}$ GeV; Bottom right: $y(0) = 0.99y_c$ with $M_{35} = 10^{5.5}$ GeV.

3.2.3 Constraints from perturbativity and VS in the $F_0 = 0$ case

As a demonstration of the impacts of perturbativity and as well VS on the model, here we assume the ideal limit for F_0 , i.e., it is exactly zero and then one can obtain the highest LP scale. For the given septuplet MDM mass 25 TeV, it means that we have to fine-tune the initial $y(0) = 0.7286422$.

We survey 3 slices of the parameter space corresponding to $\lambda_4(\Lambda) = 0.4, 0, -1$ as input, and evolve the couplings to a cutoff scale of 10^{14} GeV, just a little bit

below the highest LP scale, and then impose the VS and perturbativity conditions to give constraints. Here the perturbativity conditions mean that the absolute value of any coupling cannot exceed 4π . We assume $M_{35} = 10^{5.5}$ GeV and the results are shown in Fig. 5, where the blue (red) regions are excluded by the VS (perturbativity) conditions, while the white regions can fulfill both the conditions. These plots have the following features.

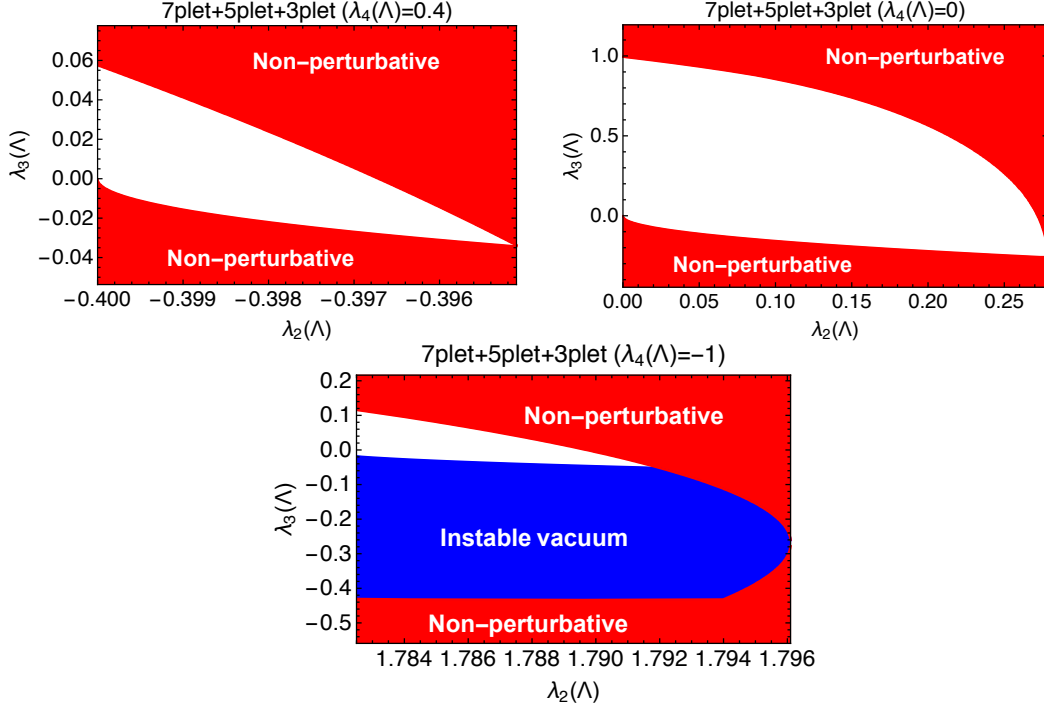


Figure 5: Regions excluded by the VS (blue) and perturbativity (red) conditions in the $\lambda_2(\Lambda)$ - $\lambda_3(\Lambda)$ plane for the 7-3-5 model. The top-left (top-right) panel corresponds to $\lambda_4(\Lambda) = 0.4$ (0), while the bottom panel corresponds to $\lambda_4(\Lambda) = -1$.

- When $\lambda_4(\Lambda) = 0.4$, the acceptable range of $\lambda_3(\Lambda)$ that fulfill the two conditions is $-0.034 \lesssim \lambda_3(\Lambda) \lesssim 0.057$. On the other hand, $\lambda_2(\Lambda)$ is bounded as $-0.4 \leq \lambda_2(\Lambda) \lesssim -0.395$, which is very narrow. 0.4 is almost the upper bound on $\lambda_4(\Lambda)$. If $\lambda_4(\Lambda)$ has a larger value, it will grow too fast and cannot keep perturbative up to the cutoff scale.
- When $\lambda_4(\Lambda) = 0$, the region survived in the $\lambda_2(\Lambda)$ - $\lambda_3(\Lambda)$ plane is maximized. The acceptable range of $\lambda_3(\Lambda)$ is $-0.247 \lesssim \lambda_3(\Lambda) \lesssim 0.995$, which is denoted by the green band in the m_0 - λ_3 plane in Fig. 1. On the other hand, the acceptable range of $\lambda_2(\Lambda)$ is enlarged as $0 \leq \lambda_2(\Lambda) \leq 0.278$. Notice that the whole perturbative region satisfies the VS conditions when $\lambda_4(\Lambda) \geq 0$.

- When $\lambda_4(\Lambda) = -1$, the range of $-0.047 < \lambda_3(\Lambda) < 0.116$ is acceptable, and $\lambda_2(\Lambda)$ is bounded by the two conditions as $1.783 \leq \lambda_2(\Lambda) \leq 1.792$, which are the maximal values that $\lambda_2(\Lambda)$ can be in the 7-3-5 model. If $\lambda_4(\Lambda)$ becomes smaller, the vacuum instability region will enlarge and leave no more acceptable region. Therefore, -1 is basically the lower bound on $\lambda_4(\Lambda)$.

In order to further understand these results, we present an analytical analysis in §3.3.1. The existence of perturbative and vacuum stable parameter regions relies on the fact that the solutions to quartic coupling RGEs could finally converge to a simple pattern in high energy scales. They are all asymptotically proportional to $g_2^2(\mu)$ and fortunately these asymptotic solutions trivially satisfy the VS conditions (23) or (24). Note that for $\lambda_4(\Lambda) < 0$ there are some regions satisfying the perturbativity conditions but excluded by the VS conditions. Even so, this is not conflict with the above statement, because these vacuum instability regions appear before the quartic couplings converge to their asymptotic solutions.

3.2.4 Towards the Planck scale: relaxing the septuplet mass

One of the main merits of the MDM model is that it predicts a unique mass for thermally produced DM particles via the observed relic abundance. But we may give it up and turn to other production mechanisms rather than the conventional freeze-out mechanism, e.g., freeze-in much lighter MDM [34]. Then, the MDM particle mass can be relaxed. For pushing up the LP scale, a much heavier MDM particle is favored. One may worry about the correct MDM relic density because heavier MDM could not quickly annihilate and thus would overclose the Universe. However, if MDM is very heavy, for instance, at PeV or even higher scales, it is reasonable to conjecture that MDM is not abundantly produced, provided that the reheating temperature is even lower than the mass scale of the MDM particle. Thus one may utilize some nonthermal ways to produce the correct relic abundance. A detailed study is beyond the scope of this paper, and we refer to some relevant studies [35, 36].

Let us consider an example with $m_0 = 10^8$ GeV. We find that M_{35} should be chosen lower than $10^{9.5}$ GeV to prevent disastrous growing behaviors of the quartic couplings. Now the LP scale can be higher than 10^{15} GeV and we should take into account the second generation triplet. Thus the running of g_2 obtains an extra correction and becomes faster. The highest LP scale, which is actually $\Lambda_{\text{LP}}^{(g_2)}$, can be determined by

$$0 = \alpha_2^{-1}(\Lambda_{\text{LP}}^{(g_2)}) = \alpha_2^{-1}(m_Z) - \frac{b_2^{\text{SM}}}{2\pi} \ln \frac{\Lambda}{m_Z} - \frac{b_2^{\text{sep}}}{2\pi} \ln \frac{\Lambda_1}{\Lambda} - \frac{b_2^{(1)}}{2\pi} \ln \frac{\Lambda_2}{\Lambda_1} - \frac{b_2^{(2)}}{2\pi} \ln \frac{\Lambda_{\text{LP}}^{(g_2)}}{\Lambda_1}, \quad (57)$$

where $b_2^{(1)} = 19/2$ and $b_2^{(2)} = 65/6$. Λ_1 (Λ_2) corresponds to the threshold scale of the first (second) generation triplet. The numerical result is $\Lambda_{\text{LP}}^{(g_2)} \simeq 10^{21}$ GeV, which is higher than the Planck scale. Then even in the $F_0 \neq 0$ case for $y_{(2)}(\Lambda_2)$ (the Yukawa coupling for the second generation triplet), the model is still possible to remain perturbative up to the Planck scale.

3.3 Analytical treatments

3.3.1 $F_0 = 0$

In the special case of $F_0 = 0$, the evolution of $y(t)$ exactly follows that of $g_2(t)$, and we can reach the maximal LP scale $\Lambda_{\text{LP}}^{(g_2)}$. Although there is no particular theoretical motivation, it would be illustrative to investigate such an ideal case.

If $F_0 = 0$, from Eq. (53) one gets a simple solution $y^2(t) = (24 + b_2)g_2^2(t)/25$. Substitute $y^2(t)$ into the beta functions of λ_i and λ and neglect the subdominant contributions from y_t and g_1 , we obtain the following RGEs:

$$\frac{d\lambda_2}{dt'} = 30\lambda_2^2 + \frac{45}{2}\lambda_4^2 + 51\lambda_2\lambda_4 - \frac{452}{5}g_2^2\lambda_2 - \frac{121203}{1250}g_2^4 + 2\lambda_3^2, \quad (58)$$

$$\frac{d\lambda_4}{dt'} = \frac{72264}{625}g_2^4 - \frac{452}{5}g_2^2\lambda_4 + \frac{255}{8}\lambda_4^2 + 24\lambda_2\lambda_4, \quad (59)$$

$$\frac{d\lambda_3}{dt'} = 36g_2^4 + \lambda_3 \left[-\frac{497}{10}g_2^2 + 18\lambda_2 + 4\lambda_3 + \frac{51}{2}\lambda_4 + 12\lambda \right], \quad (60)$$

$$\frac{d\lambda}{dt'} = 24\lambda^2 + \frac{9}{8}g_2^4 - 9\lambda g_2^2 + \frac{7}{2}\lambda_3^2. \quad (61)$$

We have rescaled $t' = t/16\pi^2$ to drop the annoying factor $16\pi^2$ for simplicity.

It is interesting to notice that these differential equations admit a particular solution where all couplings follow the running of $g_2^2(t')$ ⁹:

$$\lambda_2(t') = a_1 g_2^2(t'), \quad \lambda_4(t') = a_2 g_2^2(t'), \quad \lambda_3(t') = a_3 g_2^2(t'), \quad \lambda(t') = a_4 g_2^2(t'), \quad (62)$$

where all a_i are constant. Substitute them into Eqs. (58)–(61), and these differential equations become algebraic equations:

$$2b_2 a_1 = 30a_1^2 + \frac{45}{2}a_2^2 + 51a_1 a_2 - \frac{452}{5}a_1 - \frac{121203}{1250} + 2a_3^2, \quad (63)$$

$$2b_2 a_2 = \frac{72264}{625} - \frac{452}{5}a_2 + \frac{255}{8}a_2^2 + 24a_1 a_2, \quad (64)$$

$$2b_2 a_3 = 36 + a_3 \left[-\frac{497}{10} + 18a_1 + \frac{51}{2}a_2 + 4a_3 + 12a_4 \right], \quad (65)$$

⁹Here the key points are $dg_2/dt' \propto g_2^3$ and the RGEs essentially only involve scalar quartic couplings. In this sense, such solutions are generic for the scalar system with gauge interactions.

$$2b_2a_4 = 24a_4^2 + \frac{9}{8} - 9a_4 + \frac{7}{2}a_3^2. \quad (66)$$

There are two sets of solutions,

$$(a_1, a_2, a_3, a_4) = (-0.826831, 1.33252, 1.05752, 0.944318), \quad (67)$$

$$(a_1, a_2, a_3, a_4) = (-0.839066, 1.32379, 0.795673, 0.134918). \quad (68)$$

Both of them satisfy the VS conditions. The second solution, which gives a small coefficient of λ , is closer to the exact numerical result and thus will be used.

In the above treatment we do not refer to initial conditions, so it is not a surprise that they are only suitable for describing the evolution of couplings at sufficiently high energy scales, where the influence of initial conditions has been almost erased. This is closely related to the fact that $g_2(t')$ steadily increases towards high energy scales after the septuplet is involved to make $b_2 > 0$. To visualize this behavior, we demonstrate a comparison between the solutions from exact numerical calculation and from the approximate analytical solutions in Fig. 6. We can see that although some parameters are far away from the analytical solutions at the beginning, they all converge to these solutions at high energy scales.

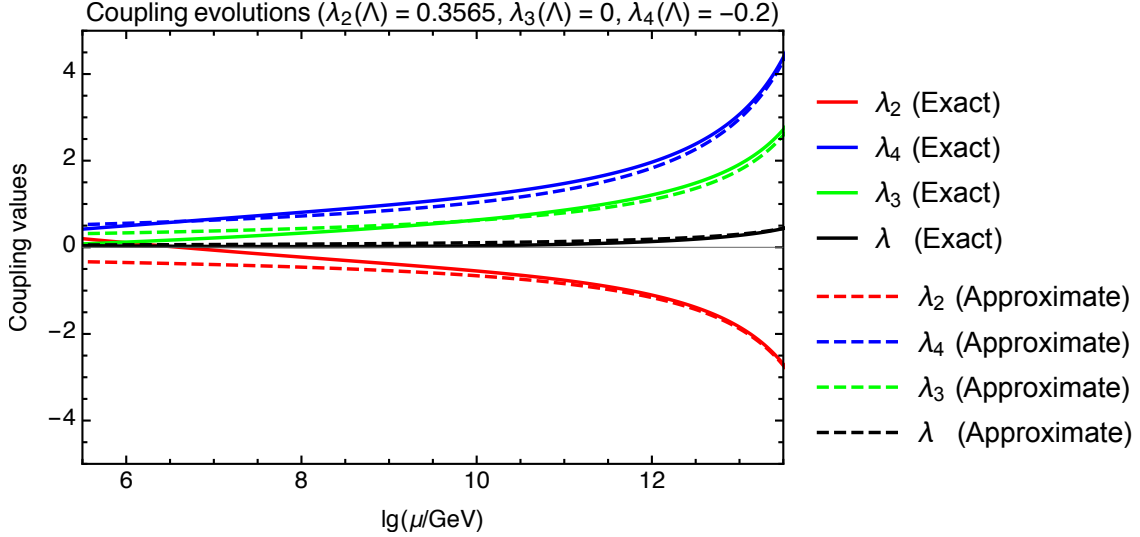


Figure 6: Evolution of λ_2 , λ_3 , λ_4 , and λ in the 7-3-5 model for $M_{35} = 10^{5.5}$ GeV. The solid lines are the exact numerical solutions, while the dashed lines represent the approximate analytical solutions based on the assumption (62).

3.3.2 $F_0 > 0$

When $F_0 > 0$, the Landau pole of y no longer exists. Instead, y becomes a non-monotonic function of the energy scale μ . It increases in the interval

$$M_{35} \leq \mu < M_{35} \exp \left\{ \frac{8\pi^2}{b_2 g_2^2(0)} \left[1 - \left(\frac{24F_0}{25b_2} \right)^{b_2/(24+b_2)} \right] \right\} \quad (69)$$

and decreases in the interval

$$M_{35} \exp \left\{ \frac{8\pi^2}{b_2 g_2^2(0)} \left[1 - \left(\frac{24F_0}{25b_2} \right)^{\frac{b_2}{24+b_2}} \right] \right\} \leq \mu < \Lambda_{\text{LP}}^{(g_2)}. \quad (70)$$

In the latter interval, y^2 behaves as

$$\frac{24 + b_2}{F_0} \left(\frac{g_2(t')}{g_2(t'_0)} \right)^{-48/b_2} g_2^2(t'_0)$$

when $g_2^2 \gg g_2^2(t'_0)$. It decrease very quickly and finally goes to zero. Then the 7-3-5 model essentially turns back to the SM+septuplet model at high energy scales. As we known, λ_2 and λ_4 will grow faster than g_2^2 and reach their Landau poles before $\Lambda_{\text{LP}}^{(g_2)}$. To illustrate this more concretely, we will solve the RGEs at high energy scales. The equations are

$$\frac{d(g_2^2)}{dt'} = 2b_2 g_2^4 \quad \text{with} \quad b_2 = \frac{19}{2}, \quad (71)$$

$$\frac{d\lambda_2}{dt'} = 30\lambda_2^2 + \frac{45}{2}\lambda_4^2 + 51\lambda_2\lambda_4 - 144g_2^2\lambda_2, \quad (72)$$

$$\frac{d\lambda_4}{dt'} = 288g_2^4 + \frac{255}{8}\lambda_4^2 + 24\lambda_2\lambda_4 - 144g_2^2\lambda_4. \quad (73)$$

We have neglected the $2\lambda_3^2$ term in Eq (72) but it would not affect the result a lot.

The things we would like to do is similar to the treatment in Ref. [17], but we include the running effect of g_2 rather than treat g_2 as constant. We assume that

$$\lambda_2(t') = f_1(t')g_2^2(t'), \quad \lambda_4(t') = f_2(t')g_2^2(t'), \quad (74)$$

where $f_{1,2}(t')$ are some functions of t' . Substitute them into Eqs. (72)–(73), and we find

$$\frac{df_1}{dG} = 30f_1^2 + \frac{45}{2}f_2^2 + 51f_1f_2 - (144 + 2b_2)f_1, \quad (75)$$

$$\frac{df_2}{dG} = 288 + \frac{255}{8}f_2^2 + 24f_1f_2 - (144 + 2b_2)f_2. \quad (76)$$

where $dG = g_2^2(t')dt'$. The function G can be easily obtained by integration and the result is

$$G(t') = \frac{1}{b_2} \ln \left(\frac{g_2(t')}{g_2(t'_0)} \right). \quad (77)$$

The right hand side of Eq. (75) does not contain a constant, but the right hand side of Eq. (76) does.

We treat these equations in a way similar to what was did in Ref. [17]. Firstly, redefine f_2 to remove the $24f_1f_2$ term. This can be done by linearly combining f_1 and f_2 as $F = f_1 + \eta f_2$ with $\eta = (17 + \sqrt{7968})/64 \approx 1.66046$. Then the equation of F is

$$\frac{dF}{dG} = c_0 - c_1F + c_2F^2 + c'f_1^2, \quad (78)$$

where

$$c_0 = 288\eta \approx 478.212, \quad c_1 = 144 + 2b_2 = 163, \quad (79)$$

$$c_2 = \frac{12(153 + \sqrt{7969})}{\sqrt{7969} + 17} \approx 27.3572, \quad c' = 30 - c_2 \approx 2.64278. \quad (80)$$

The effect of $c'f_1^2$ in Eq. (78) can be neglected because c' is small, and we can analytically solve the equation. The solution is

$$F(t') = \frac{c_1}{2c_2} + \hat{d} \tan \left\{ c_2 \hat{d} G(t') + \tan^{-1} \left[\frac{1}{\hat{d}} \left(F(t'_0) - \frac{c_1}{2c_2} \right) \right] \right\}, \quad (81)$$

with

$$\hat{d} = \sqrt{\frac{c_0}{c_2} - \frac{c_1^2}{4c_2^2}} \approx 2.93346. \quad (82)$$

Here t'_0 is chosen to correspond to a scale Λ_0 where $y(t'_0)$ is small compared to $g_2(t'_0)$. We can see that $F(t')$ diverges when

$$c_2 \hat{d} G(t') + \tan^{-1} \left[\frac{1}{\hat{d}} \left(F(t'_0) - \frac{c_1}{2c_2} \right) \right] = \frac{\pi}{2}.$$

It means for any initial value of $F(t'_0)$, there always exists a Landau pole of $F(t')$ with a finite value of $G(t')$. This LP scale is

$$\begin{aligned} \Lambda_{\text{LP}}^{(F)} &= \Lambda_0 \exp \left\{ \frac{8\pi^2}{b_2 g_2^2(t_0)} \left[1 - \exp \left(-\frac{b_2 \pi}{c_2 \hat{d}} \left[1 - \frac{2}{\pi} \tan^{-1} \left(\frac{F(t'_0)}{\hat{d}} - \frac{c_1}{2c_2 \hat{d}} \right) \right] \right) \right] \right\} \\ &= \Lambda_{\text{LP}}^{(g_2)} \exp \left[-\frac{8\pi^2}{b_2 g_2^2(t'_0)} \exp \left(-\frac{b_2 \pi}{c_2 \hat{d}} \left[1 - \frac{2}{\pi} \tan^{-1} \left(\frac{F(t'_0)}{\hat{d}} - \frac{c_1}{2c_2 \hat{d}} \right) \right] \right) \right]. \quad (83) \end{aligned}$$

If we choose the range of $y(0)$ satisfying $25y_c^2/26 \leq y^2(0) < y_c^2$ to make $0 < F_0 \leq 1$, we can assume that y is small enough to be ignored in the running when the ratio

$$\xi \equiv \frac{y^2(t'_0)}{(24 + b_2)g_2^2(t'_0)/25} = \left[1 + \frac{F_0}{25} \left(\frac{g_2^2(t'_0)}{g_2^2(t'_f)} \right)^{(24+b_2)/b_2} \right]^{-1}$$

is small enough. This will fix the value of $g_2(t'_0)$ by

$$\frac{1}{g_2^2(t'_0)} = \frac{1}{g_2^2(0)} \left[\frac{\xi F_0}{25(1 - \xi)} \right]^{b_2/(24+b_2)}. \quad (84)$$

Notice that from the scale M_{35} to the scale Λ_0 , the function of $y(t)$ can be approximated by that in the $F_0 = 0$ limit. This means that in this scale range, the approximate solutions of λ_i and λ to Eqs. (62) work well if Λ_0 is high enough. Then we can estimate $F(t'_0)$ by $a_1 + \eta a_2 \approx 1.359$, and the LP scale is

$$\Lambda_{\text{LP}}^{(F)} \approx \Lambda_{\text{LP}}^{(g_2)} \exp \left[-\frac{8\pi^2}{b_2 g_2^2(0)} \left(\frac{\xi F_0}{25(1 - \xi)} \right)^{b_2/(24+b_2)} \times \exp \left(-\frac{b_2 \pi}{c_2 \hat{d}} \left[1 - \frac{2}{\pi} \tan^{-1} \left(\frac{a_1 + \eta a_2 - c_1/(2c_2)}{\hat{d}} \right) \right] \right) \right]. \quad (85)$$

For $F_0 \leq 1$, $\xi = 0.895$ leads to an agreement with the full numerical calculation. We show the ratio $\Lambda_{\text{LP}}^{(g_2)}/\Lambda_{\text{LP}}^{(F)}$ as a function of F_0 in Fig. 7. We can see that for $F_0 = 1$, the LP scale of F is smaller than $\Lambda_{\text{LP}}^{(g_2)}$ by 4 orders of magnitude. If one wants $\Lambda_{\text{LP}}^{(F)}$ to be $\sim 10^{-1}\Lambda_{\text{LP}}^{(g_2)}$, F_0 should be tuned to ~ 0.002 , which is unnatural. For a larger F_0 , $\Lambda_{\text{LP}}^{(F)}$ is lower, because the 7-3-5 Yukawa coupling has smaller effect on the running of quartic couplings.

4 Conclusions and discussions

Perturbativity yields strong bounds on the MDM model, but most of the previous studies only consider the gauge couplings and conclude that the real scalar septuplet MDM model can keep perturbative up to the Planck scale. In this article we take into account the quartic self-interactions of the real scalar septuplet in the septuplet MDM model, and find that for an MDM particle mass of ~ 10 TeV the Landau poles of the quartic couplings appear around 10^8 GeV, which is consistent with the approximate analytical treatment in Ref. [17].

As an attempt to push up the LP scale, we propose an extension to the model with Yukawa interactions among the septuplet, an extra fermionic quintuplet, and one or two extra fermionic triplets. In principle, the Landau pole can be deferred

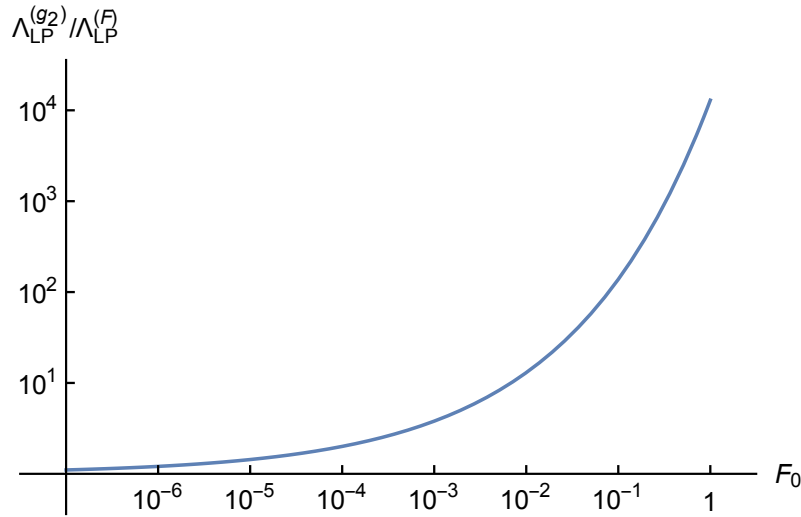


Figure 7: The ratio $\Lambda_{LP}^{(g_2)}/\Lambda_{LP}^{(F)}$ as a function of F_0 in the range $0 < F_0 \leq 1$.

to appear at 10^{14} GeV, but it is at the price of a serious fine-tuning of the initial condition of the new Yukawa coupling. We investigate the evolution of couplings up to a scale just a little bit below the highest possible LP scale, and use the VS and perturbativity conditions to constrain the quartic couplings. It is found that the Higgs portal coupling has an acceptable range of $-0.25 < \lambda_3 < 1$. Moreover, if the MDM particle mass could be relaxed to $\sim 10^8$ GeV, which demands some nonthermal production mechanisms, we could push up the LP scale even beyond the Planck scale.

In a scalar MDM model with doublet, triplet, or quadruplet, the couplings can remain perturbative up to the Planck scale. On the other hand, when the MDM scalar multiplet lives in an $SU(2)_L$ representation with a dimension higher than 5, the scalar MDM model would have Landau poles appearing before the Planck scale, due to the MDM framework, i.e., the MDM particle mass fixed by thermal freeze-out dynamics. As what we propose in this article, these models may be cured as well by introducing extra Yukawa couplings. We leave this possibility to a specific study [37].

Acknowledgments

This work is supported by the National Natural Science Foundation of China (NSFC) under Grant Nos. 11375277, 11410301005, and 11005163, the Fundamental Research Funds for the Central Universities, and the Sun Yat-Sen University Science Foundation.

References

- [1] M. Cirelli, N. Fornengo and A. Strumia, *Minimal dark matter*, Nucl. Phys. B **753**, 178 (2006) [hep-ph/0512090].
- [2] M. Cirelli, A. Strumia and M. Tamburini, *Cosmology and Astrophysics of Minimal Dark Matter*, Nucl. Phys. B **787**, 152 (2007) [arXiv:0706.4071 [hep-ph]].
- [3] M. Cirelli and A. Strumia, *Minimal Dark Matter: Model and results*, New J. Phys. **11**, 105005 (2009) [arXiv:0903.3381 [hep-ph]].
- [4] T. Hambye, F.-S. Ling, L. Lopez Honorez and J. Rocher, *Scalar Multiplet Dark Matter*, JHEP **0907**, 090 (2009) [Erratum-ibid. **1005**, 066 (2010)] [arXiv:0903.4010 [hep-ph]].
- [5] F. S. Ling, *Heavy Scalar Dark Matter*, arXiv:0905.4823 [hep-ph].
- [6] K. Earl, K. Hartling, H. E. Logan and T. Pilkington, *Constraining models with a large scalar multiplet*, Phys. Rev. D **88**, 015002 (2013) [arXiv:1303.1244 [hep-ph]].
- [7] M. Cirelli, R. Franceschini and A. Strumia, *Minimal Dark Matter predictions for galactic positrons, anti-protons, photons*, Nucl. Phys. B **800**, 204 (2008) [arXiv:0802.3378 [hep-ph]].
- [8] M. Cirelli and A. Strumia, *Minimal Dark Matter predictions and the PAMELA positron excess*, PoS IDM **2008**, 089 (2008) [arXiv:0808.3867 [astro-ph]].
- [9] M. Cirelli, T. Hambye, P. Panci, F. Sala and M. Taoso, *Gamma ray tests of Minimal Dark Matter*, arXiv:1507.05519 [hep-ph].
- [10] C. Garcia-Cely, A. Ibarra, A. S. Lamperstorfer and M. H. G. Tytgat, *Gamma-rays from Heavy Minimal Dark Matter*, arXiv:1507.05536 [hep-ph].
- [11] M. R. Buckley, L. Randall and B. Shuve, *LHC Searches for Non-Chiral Weakly Charged Multiplets*, JHEP **1105**, 097 (2011) [arXiv:0909.4549 [hep-ph]].
- [12] Y. Cai, W. Chao and S. Yang, *Scalar Septuplet Dark Matter and Enhanced $h \rightarrow \gamma\gamma$ Decay Rate*, JHEP **1212**, 043 (2012) [arXiv:1208.3949 [hep-ph]].
- [13] M. Cirelli, F. Sala and M. Taoso, *Wino-like Minimal Dark Matter and future colliders*, JHEP **1410**, 033 (2014) [JHEP **1501**, 041 (2015)] [arXiv:1407.7058 [hep-ph]].

- [14] K. Harigaya, K. Ichikawa, A. Kundu, S. Matsumoto and S. Shirai, *Indirect Probe of Electroweak-Interacting Particles at Future Lepton Colliders*, JHEP **1509**, 105 (2015) [arXiv:1504.03402 [hep-ph]].
- [15] B. Ostdiek, *Constraining the minimal dark matter fiveplet with LHC searches*, arXiv:1506.03445 [hep-ph].
- [16] L. Di Luzio, R. Grber, J. F. Kamenik and M. Nardecchia, *Accidental matter at the LHC*, JHEP **1507**, 074 (2015) [arXiv:1504.00359 [hep-ph]].
- [17] Y. Hamada, K. Kawana and K. Tsumura, *Landau pole in the Standard Model with weakly interacting scalar fields*, Phys. Lett. B **747**, 238 (2015) [arXiv:1505.01721 [hep-ph]].
- [18] R. Foot, H. Lew, X. G. He and G. C. Joshi, *Seesaw Neutrino Masses Induced by a Triplet of Leptons*, Z. Phys. C **44**, 441 (1989).
- [19] P. A. R. Ade *et al.* [Planck Collaboration], *Planck 2015 results. XIII. Cosmological parameters*, arXiv:1502.01589 [astro-ph.CO].
- [20] J. R. Ellis, A. Ferstl and K. A. Olive, *Reevaluation of the elastic scattering of supersymmetric dark matter*, Phys. Lett. B **481**, 304 (2000) [hep-ph/0001005].
- [21] D. S. Akerib *et al.* [LUX Collaboration], *First results from the LUX dark matter experiment at the Sanford Underground Research Facility*, Phys. Rev. Lett. **112**, 091303 (2014) [arXiv:1310.8214 [astro-ph.CO]].
- [22] M. Cirelli *et al.*, *PPPC 4 DM ID: A Poor Particle Physicist Cookbook for Dark Matter Indirect Detection*, JCAP **1103**, 051 (2011) [JCAP **1210**, E01 (2012)] [arXiv:1012.4515 [hep-ph]].
- [23] M. Ackermann *et al.* [Fermi-LAT Collaboration], *Searching for Dark Matter Annihilation from Milky Way Dwarf Spheroidal Galaxies with Six Years of Fermi-LAT Data*, arXiv:1503.02641 [astro-ph.HE].
- [24] K. Kannike, *Vacuum Stability Conditions From Copositivity Criteria*, Eur. Phys. J. C **72**, 2093 (2012) [arXiv:1205.3781 [hep-ph]].
- [25] T. P. Cheng, E. Eichten and L. F. Li, *Higgs Phenomena in Asymptotically Free Gauge Theories*, Phys. Rev. D **9**, 2259 (1974).
- [26] F. Lyonnet, I. Schienbein, F. Staub and A. Wingerter, *PyR@TE: Renormalization Group Equations for General Gauge Theories*, Comput. Phys. Commun. **185**, 1130 (2014) [arXiv:1309.7030 [hep-ph]].

- [27] J. Beringer *et al.* [Particle Data Group Collaboration], *Review of Particle Physics*, Phys. Rev. D **86** (2012) 010001.
- [28] T. Hambye and K. Riesselmann, *Matching conditions and Higgs mass upper bounds revisited*, Phys. Rev. D **55**, 7255 (1997) [hep-ph/9610272].
- [29] Y. Cai, X. G. He, M. Ramsey-Musolf and L. H. Tsai, *$R\nu$ MDM and Lepton Flavor Violation*, JHEP **1112**, 054 (2011) [arXiv:1108.0969 [hep-ph]].
- [30] K. Kumericki, I. Picek and B. Radovic, *Critique of Fermionic $R\nu$ MDM and its Scalar Variants*, JHEP **1207**, 039 (2012) [arXiv:1204.6597 [hep-ph]].
- [31] P. Culjak, K. Kumericki and I. Picek, *Scotogenic $R\nu$ MDM at three-loop level*, Phys. Lett. B **744**, 237 (2015) [arXiv:1502.07887 [hep-ph]].
- [32] E. Witten, *An $SU(2)$ Anomaly*, Phys. Lett. B **117** (1982) 324.
- [33] O. Bar, *On Witten's global anomaly for higher $SU(2)$ representations*, Nucl. Phys. B **650** (2003) 522 [hep-lat/0209098].
- [34] M. Aoki, T. Toma and A. Vicente, *Non-thermal Production of Minimal Dark Matter via Right-handed Neutrino Decay*, arXiv:1507.01591 [hep-ph].
- [35] D. J. H. Chung, E. W. Kolb and A. Riotto, *Superheavy dark matter*, Phys. Rev. D **59**, 023501 (1999) [hep-ph/9802238].
- [36] A. Falkowski and J. M. No, *Non-thermal Dark Matter Production from the Electroweak Phase Transition: Multi-TeV WIMPs and 'Baby-Zillas'*, JHEP **1302**, 034 (2013) [arXiv:1211.5615 [hep-ph]].
- [37] C. Cai, Z. M. Huang, Z. Kang, Z. H. Yu and H. H. Zhang, in preparation.